

Closing report of the OTKA-K100196 grant

Period: 01.01.2012 - 31.12.2015.

Title of the project: Generation of a genetically engineered total PPAR γ null mouse line, a new model to study the function of the receptor

A project magyar címe: Egy új PPAR γ null egértörzs létrehozása, a receptor működésének tanulmányozására

The aim of this project:

The fatty acid activated transcription factor PPAR γ (peroxisome proliferator-activated receptor gamma) has been linked to adipocyte differentiation, macrophage and dendritic cell function and also to diseases such as diabetes, atherosclerosis and chronic inflammation. However assigning cellular functions to the receptor in various cell types has been hampered by the lack of appropriate genetic models in which PPAR γ is completely eliminated from a given cell type or an entire animal. In this proposal we aimed to developed and characterized a complete PPAR γ null mouse line and also bone marrow chimeras. We also aimed to generate embryonic fibroblasts and induced pluripotent stem cells from these mice to allow investigations of the cellular role of this transcription factor in physiological and pathophysiological processes.

Generation and characterization of PPAR γ null mice.

PPAR γ deficiency results in embryonic lethality. To solve this problem, we have crossed PPAR γ floxed mice with Sox2Cre mice, where the Sox2 promoter driven Cre generates a complete excision in epiblast cells, therefore, all embryonic tissues will lack of PPAR γ expression (Figure 1).

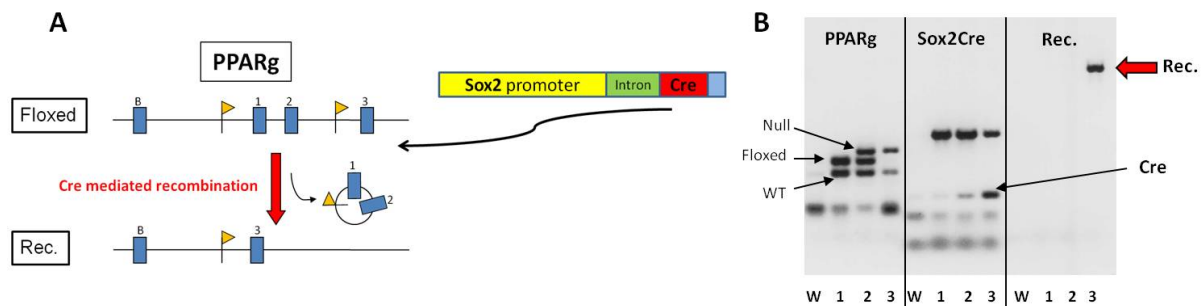


Figure 1. A) Excision of floxed PPAR γ allele due to the Cre recombinase driven by Sox2 promoter. B) Determination of genotypes by agarose gel electrophoresis. (W = water control, 1 = PPAR γ ^{fl/+}Cre⁻, 2 = PPAR γ ^{fl/-}Cre⁻, 3 = PPAR γ ^{Δfl/-}Cre⁺ recombined flox allele).

The PPAR γ knockout (KO) mice show several phenotypic differences, such as lack of white and brown adipose tissues, enlarged fatty liver, organomegaly, dry and inflexible skin, undeveloped genital organs (Figure 2). Histological characterization shows further abnormalities such as steatohepatitis, lack of sebaceous glands in the skin and pancreatic beta islands hypertrophy. In case of phenotypic abnormalities these mice are very sensitive for environmental conditions such as temperature, quality of food and nesting materials. Most of PPAR γ null neonates die in conventional conditions and sometimes its own mother selected them out and killed them. We have used several resources to adjust the best conditions in our animal house where several PPAR γ null mice survive and reach adulthood. We have to

maintain a big mouse colony with around 150-200 mice to generate appropriate amount of mice for experiments.

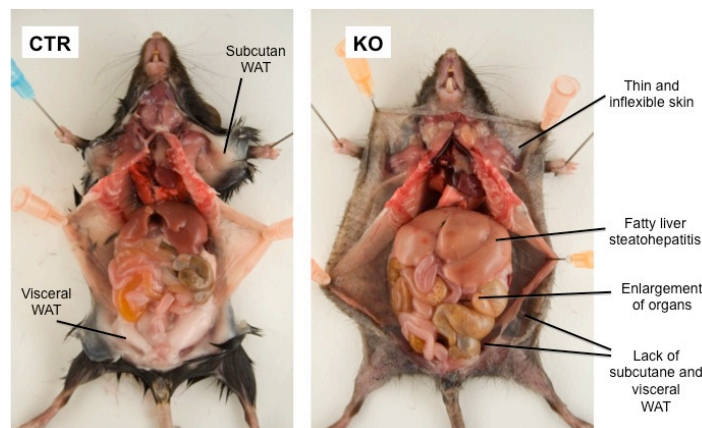


Figure 2. Phenotypic differences between control and PPARg null mice.

We characterized the metabolic parameters of these mice using our Oxymax/CLAMS (Comprehensive Laboratory Animal Monitoring System) system in which we can measure 8 mice at the same time. The results showed higher metabolic rate and reduced activity in the PPARg null mice.

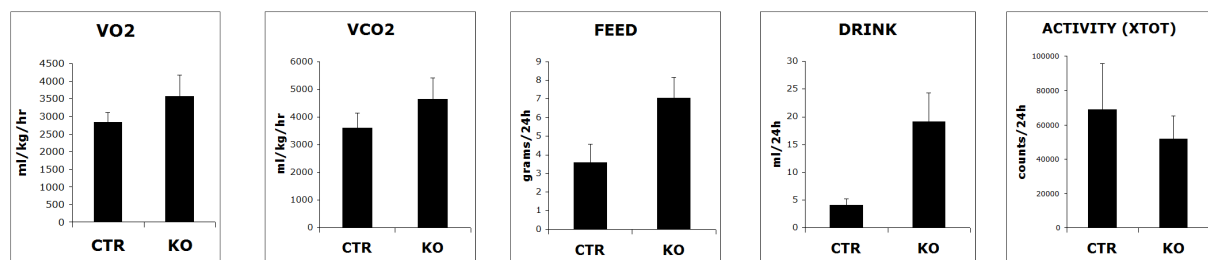


Figure 3. Phenotypic differences between control and PPARg null mice.

Some blood parameters such as lipoproteins, glucose and insulin among others showed higher levels in the KO mice. Interestingly, the leptin levels in the blood decreased, but not disappeared in spite of the lack of adipose tissue (Figure 4). It is possible that somehow the fatty liver can produce leptin.

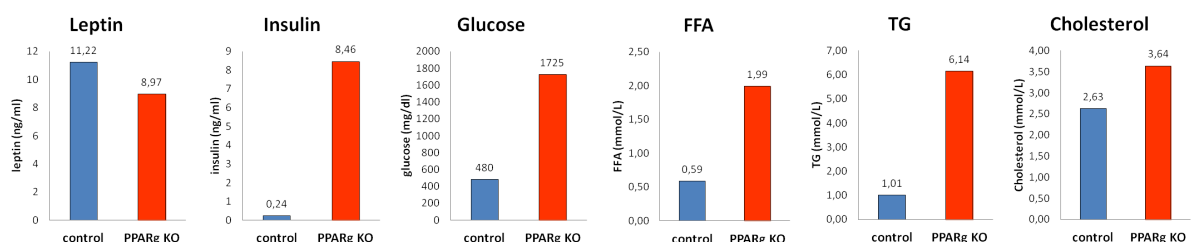


Figure 4. Measurements of plasma components (FFA = free fatty acids, TG = triglycerides).

The intraperitoneal glucose tolerance test showed insulin resistance similar to type 2 diabetes. We measured the PPARg expression in different tissues by RT-qPCR using an assay specific for the exon 2-3 of PPARg, which can demonstrate the recombination efficiency. The results show the lack of PPARg expression in the measured tissues such as liver, colon, kidney, thymus, spleen and lung. However, using another assay specific for the exon 5-6 gave

measurable expression, which suggests that, a truncated PPAR γ mRNA could be expressed, but it is not functional.

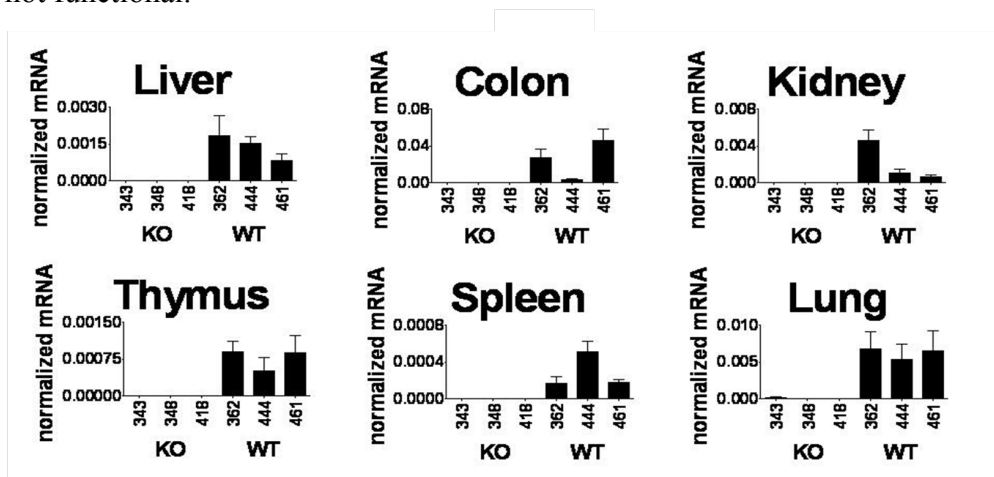


Figure 5. Expression of PPAR γ mRNA in different tissues

Generation and characterization of PPAR γ null chimeric mice.

Using bone marrow transplantation we set up a model, where lethally irradiated congenic mice were transplanted with PPAR γ null bone marrow and could generate chimeric mice, where all the hematopoietic cells will be PPAR γ null, while other tissues normally express PPAR γ . This model is a useful tool to investigate the role of PPAR γ in the differentiation and function of immune cells such as macrophages or dendritic cells.

The reason why it was difficult to maintain the PPAR γ -KO mice alive led us to set up an embryonic liver cell transplantation method, which could replace the bone marrow transplantation. The fetal liver is the main hematopoietic organ in the mouse embryo between E11-E16 days and the isolated embryonic liver cells can effectively repopulate the hematopoietic system of irradiated recipient after transplantation. We have crossed PPAR $\gamma^{+/-}$ Sox2Cre⁺ males with PPAR $\gamma^{fl/fl}$ Sox2Cre⁻ females in timed mating and after 13.5 days we sacrificed the pregnant females and isolated the embryos. There were no visible morphological difference between wild type (WT) and PPAR γ -KO (KO) embryos at this stage. We isolated the liver from each embryo and after we determined the genotypes and the genders of the embryos by PCR and RT-qPCR methods. Then we selected the PPAR $\gamma^{fl/fl}$ Sox2Cre⁺ (KO) and control C57BL/6J liver cell suspensions for the transplantation.

We lethally irradiated 8-10 weeks old BoyJ congenic recipient female mice and we transplanted with PPAR γ -KO and C57BL/6 (wild type) donor embryonic liver cells by retro-orbital injection in a gender specific manner. The mice were kept in sterile conditions in a ventilated cabinet for 8 weeks and then we detected the chimerism in all transplanted mice using flow cytometry method. We took a small drop of blood from the tail of each mouse and stained the blood leukocytes with GR-1 (granulocyte marker) and CD45.2 (leukocyte marker in the mice with C57BL/6 genetic background) markers. Gating on the granulocyte population we could measure the double positive donor cell ratio in the transplanted mice. Our results showed near 100% repopulation efficiency in all transplanted mice (Figure 7).

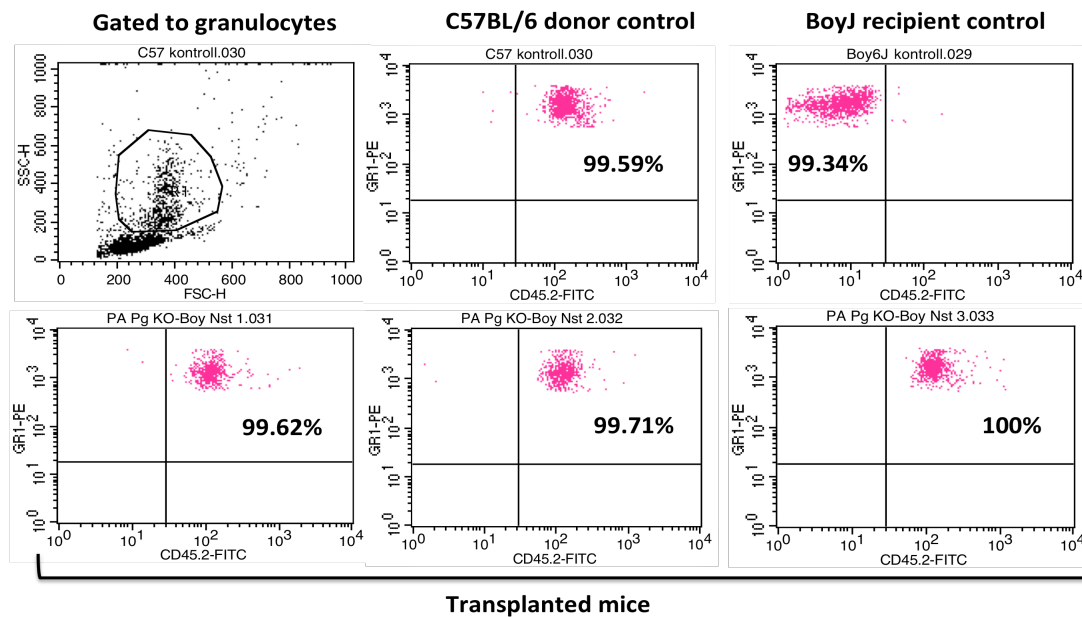


Figure 7. The repopulation effectiveness of the PPARg embryonic liver transplanted BoyJ mice.

Using the Oxymax/CLAMS system we measured the metabolic parameters of transplanted mice. The results did not show significant differences between mice transplanted with PPARg-KO or control embryonic liver cells, however the food intake and the activity were slightly reduced in the KO transplanted BoyJ mice.

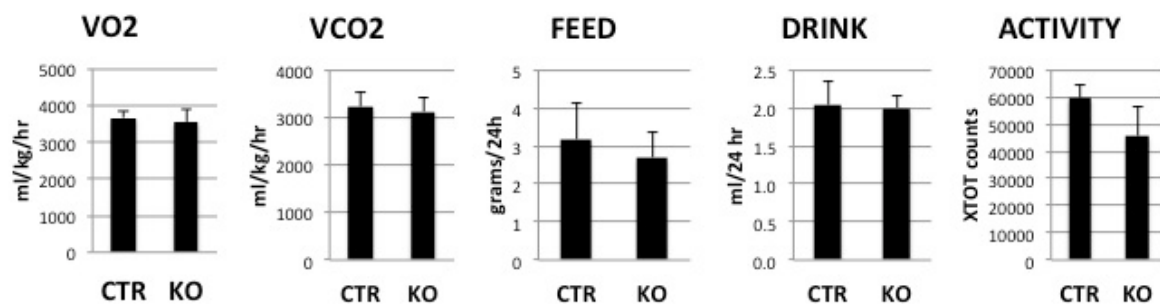


Figure 8. Metabolic characterization of BoyJ mice transplanted with control (CTR) and PPARg-KO (KO) bone marrow cells

Differentiation of macrophages from PPARg null chimeric mice and RNA-Seq measurement:

We isolated bone marrow cells from the transplanted chimera mice and differentiated macrophages using L929 cell supernatant containing M-CSF. After 6 days we culture the macrophages into serum free medium. Our previous results suggest the IL-4 could improve the effect of PPARg activation on transcription regulation, so we treated the macrophages with or without IL-4 cytokine (20 ng/ml) for 24 hours. Then we also treated the cells with or without the PPARg agonist rosiglitazone (RSG, 10^{-6} M) for 12 hours. We had 4 different treatments at the end of differentiation from each individual mouse:

- M-CSF
- M-CSF+RSG
- M-CSF+IL4
- M-CSF+IL4+RSG

We isolated total RNA from the different macrophage samples. We checked the RNA quality of all samples and measured the expression of two well-known PPAR γ target genes (Angptl4 and FABP4) by qPCR. We selected the samples from 3 control C57BL/6 and 3 PPAR γ -KO mice and used them for RNA-Seq measurement to determine the gene expression profile of these samples. The RNA-Seq results showed that the expression of exon 1 and 2 of PPAR γ gene disappears in PPAR γ -KO samples, which are correlated with our previous qPCR data. This is the region, which was recombined in the PPAR γ -KO mice.

We analyzed the RNA-Seq data using R software. We decided to analyze the IL-4 treated and untreated samples separately, because we would like to focus in the genes, which are regulated by PPAR γ deletion and by PPAR γ activation. During the analysis we filtered for 2 fold significant changes in any condition comparing the wild type and PPAR γ -KO samples.

We could detect that around 10 times more genes changed at least 2 folds by deletion of PPAR γ , in contrast to the genes regulated by PPAR γ ligand treatment (Figure 9). The overlapping genes contain those well-known PPAR γ target genes like Angptl4, Fabp4, Arg1. It means that PPAR γ can directly or indirectly regulates the expression of several genes without ligand activation. There are also genes, which are regulated by PPAR γ ligand treatment, but the deletion of PPAR γ has no effect on the expression of these genes.

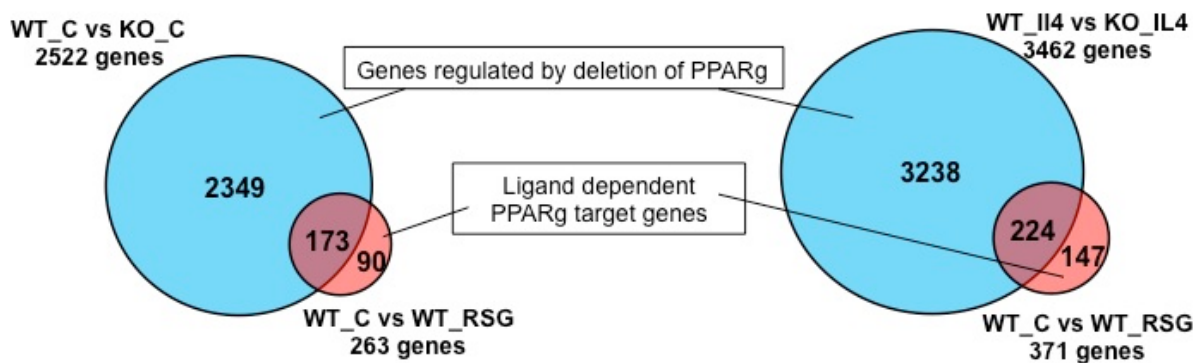


Figure 9. Analysis of the RNA-Seq results

The cluster analysis of significantly changing genes also showed that most of these genes are regulated only by PPAR γ deletion in macrophage samples both with or without IL-4 treatment (Cluster 1 and 5 on Figure 10 and Cluster 1 and 3 on Figure 11). There are clusters where ligand treatment up- or downregulates the gene expression, while PPAR γ deletion has an opposite effect. These clusters contain the potential ligand dependent PPAR γ target genes and it is important that more genes are in these clusters in case of macrophages without any IL-4 treatment (Cluster 2 and 4 on Figure 10 and Cluster 2 and 6 on Figure 11). Interestingly, there are clusters of genes, which show similar expression changes upon ligand treatment and deletion of PPAR γ receptor; this is more characteristic to the IL-4 treated alternatively activated macrophages (Cluster 3 and 6 on Figure 10 and Cluster 4 and 5 on Figure 11). These results suggest that PPAR γ regulates gene expression in more ligand sensitive manner in macrophages without IL-4 treatment, however IL-4 treatment increase the PPAR γ expression itself and enhance the expression regulation of many genes in a ligand independent manner. It is clear in all clusters that RSG has no or has only a very small effect in PPAR γ -KO samples.

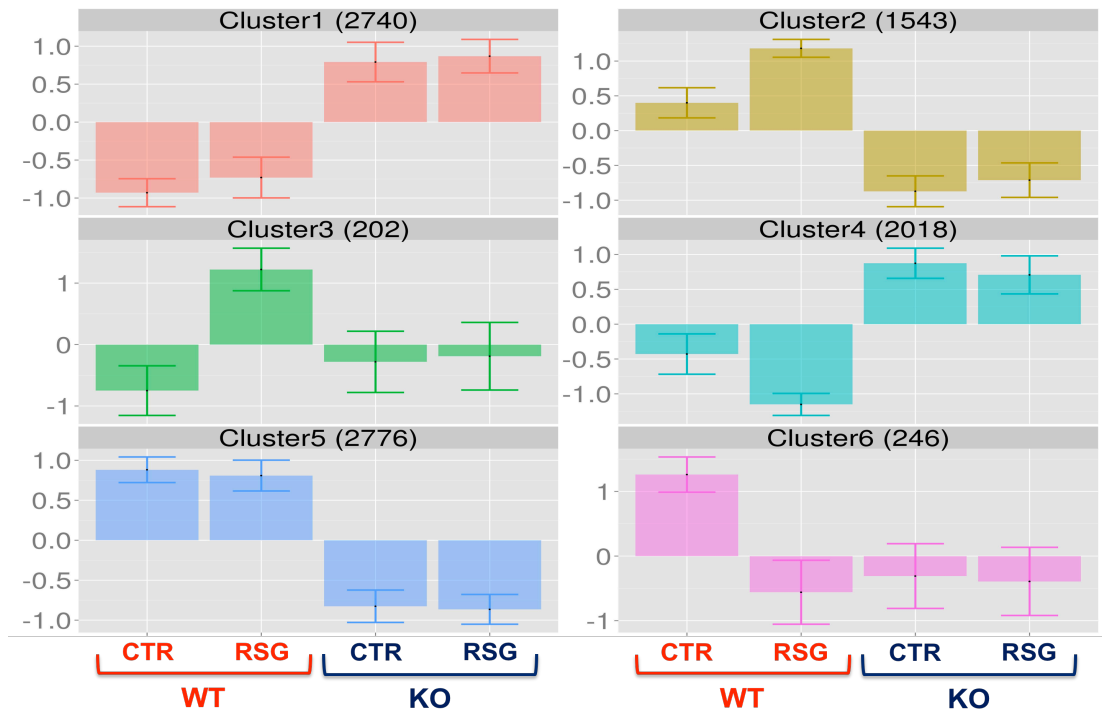


Figure 10. Clustering significantly changing genes in macrophages without IL4

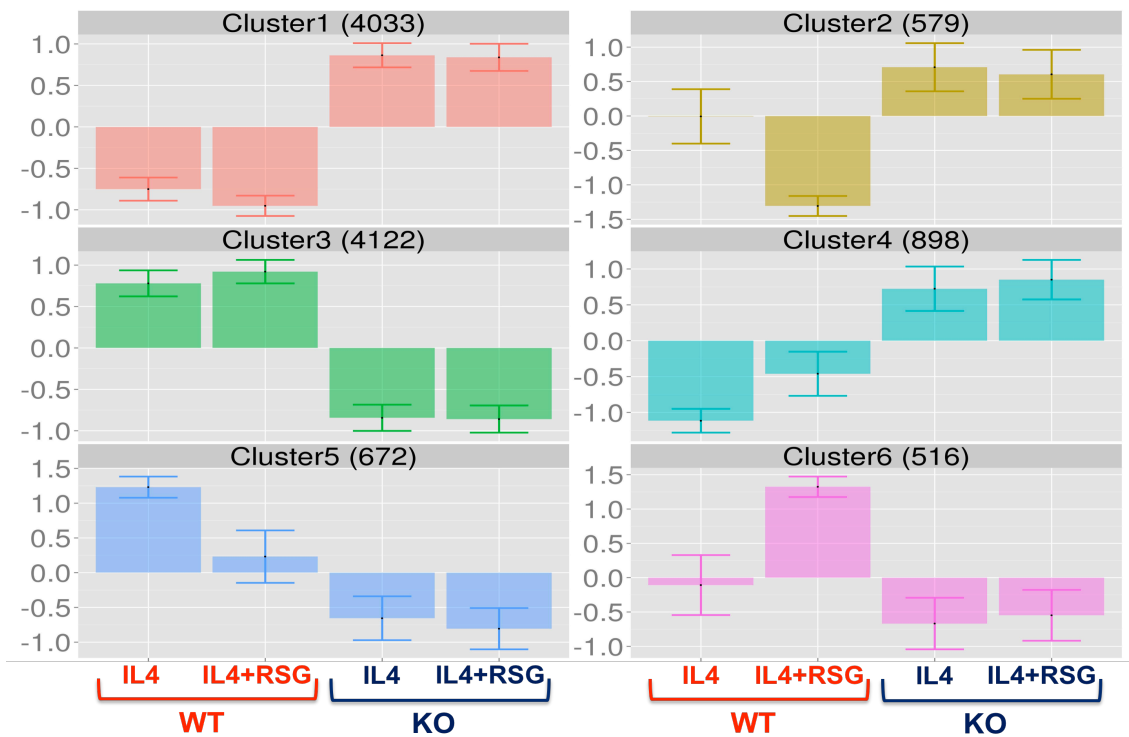


Figure 11. Clustering significantly changing genes in IL4 treated macrophages

We are interested in the biological functions of these PPAR γ regulated genes. Therefore, we used the Panther Classification System online software for the analysis. When we made the functional classification of genes that are regulated by PPAR γ deletion we got very similar results comparing the IL-4 treated and untreated macrophages. Making a rank order upon the P values the most representative categories were: cytokine receptor, defense/immunity protein, immunoglobulin receptor superfamily, signaling molecule, receptor.

We also made the same classification using the genes, which are regulated in macrophages by PPAR γ ligand treatment. In macrophages without IL-4 treatment the top categories are „antibacterial response protein” and „chemokine”, while in IL-4 treated macrophages the top categories are „signaling molecule” and „defense/immunity proteins”. These results suggest that macrophages without IL-4 can mainly recognize the pathogens or foreign antigens and start to respond to these, while IL-4 treatment can modify the gene expression in macrophages and also induces other signaling pathways. Based on our results we selected some candidate genes which seems to be regulated by PPAR γ :

- Hpgd – downregulated upon PPAR γ deletion. This enzyme is responsible for the metabolism of prostaglandins, which function in a variety of physiologic and cellular processes such as inflammation. It generates 15-keto-PGE₂, a PPAR γ agonist.
- Camsap3 – a microtubule minus end binding protein downregulated in PPAR γ -KO macrophages and upregulated by ligand treatment. It could be directly regulated by PPAR γ .
- Ch25h – slightly downregulated by ligand treatment, but highly upregulated in PPAR γ -KO samples. This gene metabolizes cholesterol and generates a bioactive cholesterol metabolite (25- hydroxycholesterol). Ch25h is also reported to be regulated by TLR4 signaling. Therefore, it is possible that upon TLR4 signaling, the differential expression of Ch25h is even more different between WT and PPAR γ KO.
- Cxcl11, Ccl12, Ccl7, Cxcl9 – these chemokines are highly upregulated in PPAR γ -KO macrophages. They are induced by IFN γ , coordinate cell movement and immune response to pathogens.

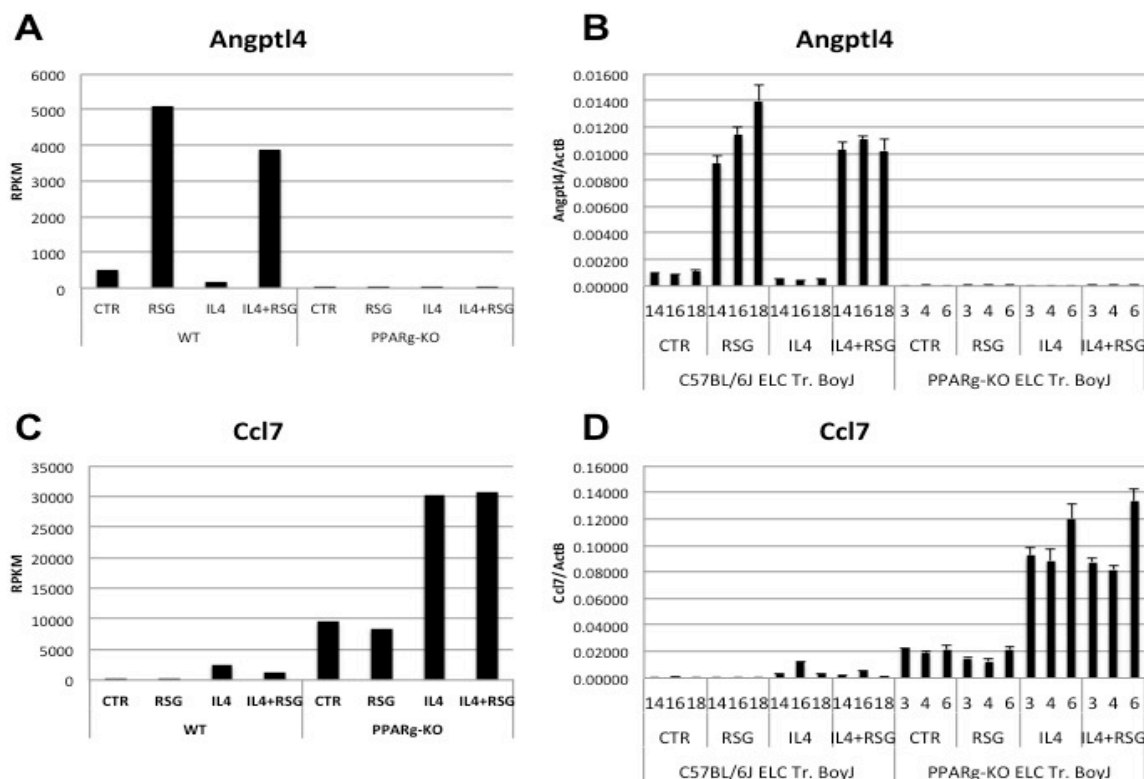


Figure 12. Validation of RNA-Seq results by qPCR. RNA-Seq (A and C) and qPCR results (B and D) were measured from the same samples, but the RNA-Seq diagrams show the average of three samples in each condition.

We successfully validated these genes by qPCR. As an example we show the known PPARg target gene *Angptl4* as a downregulated gene by PPARg deletion and a chemokine *Ccl7* as an upregulated gene in the PPARg-KO macrophages (Figure 12). Then we made a comparison of bone marrow-derived macrophages differentiated from PPARg-KO mice, PPARg-KO embryonic liver cell transplanted BoyJ mice and macrophage specific PPARg^{fl/fl}LysMCre mice and the appropriate controls. The results show that *Angptl4* and *Arg1* show similar expression pattern in all three genetic models, however *Ccl7* and *Ch25h* expressed a slightly differences in the macrophages differentiated from PPARg^{fl/fl}LysMCre mice, but seems to be similar in full body PPARg-KO and transplanted mice. This difference may be caused by the incomplete recombination of floxed alleles in PPARg^{fl/fl}LysMCre mice and also suggests that the transplanted mice are a useful model to investigate PPARg null macrophages.

Generation of immortalized bone marrow-derived macrophage cell line (iBMDM).

By the reason of difficulties to generate primary BMDMs from PPARg-KO mice we decided to generate immortalized macrophage cell lines for *in vitro* experiments. Bone marrow-derived cells were immortalized using the J2 cell line continuously producing the J2 virus encoding v-raf and v-myc oncogenes. J2 cells were grown in DMEM containing 20% FBS. Bone marrow cells were seeded in immortalization media I. (90% J2 supernatant, 5% HyClone FBS, 10ug/ml Polybrene 0.1%, L929 supernatant 5%) and incubated overnight. On the second day supernatant was collected and spin down to pellet floating cells. Adherent cells were scraped and re-plated in a new petri dish using immortalization media II. (20% J2 supernatant, 10% HyClone FBS, 10ug/ml Polybrene 0.1%, L929 supernatant 10%, 60% DMEM) and incubated for 6 days. After the immortalization cells were kept in regular macrophage differentiation media and treated with IL-4 and RSG. We measured PPARg target genes *Fabp4* and *Angptl4* to make sure that these iBMDM cell lines preserve the main features of primary cells (Figure 13).

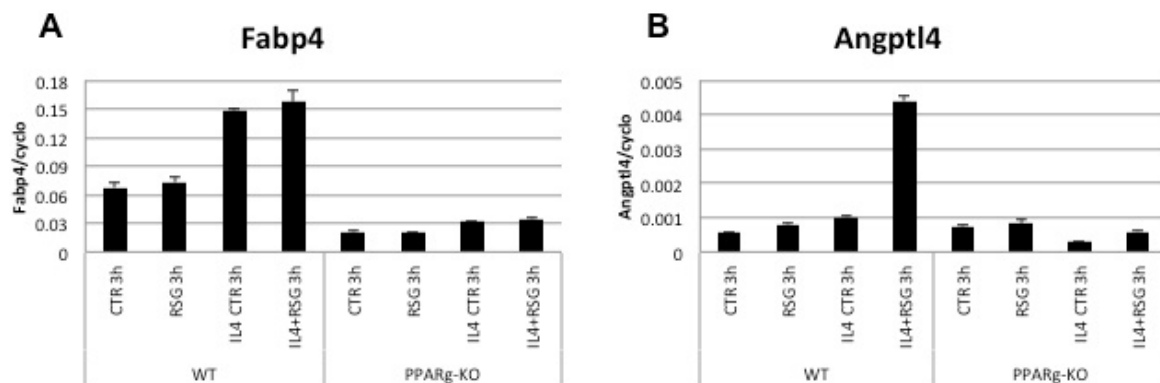


Figure 13. Measurements of PPARg target genes FABP4 (A) and Angptl4 (B) by RT-qPCR.

The results suggest that PPARg expression is very low in iBMDMs and short time ligand treatment is not enough to induce the expression of target genes, however IL-4 treatment can improve the PPARg ligand activation and this effect is disappear in PPARg-KO cell lines.

Isolation of primary mouse embryonic fibroblasts (PMEF's) from Sox2Cre PPARg mice.

In order to generate the iPS cells, PMEF's were isolated from three mothers with a total of 20 embryos. Since the embryos are different genotype background within the mother due to the Sox2Cre approach, each embryo was genotyped and treated separately. Two embryos were

PPARg knockout (PPARg^{Δfl/-}Sox2Cre⁺) and five were PPARg heterozygous control (PPARg^{fl/-}Sox2Cre⁻). The isolated PMEF's were expanded and characterized. Adipocyte differentiation from PPARg KO and control PMEF's showed the absence of adipocytes in PPARg KO cultures, meanwhile in the control PMEF's, Oil red O staining and qPCR for adipocyte specific markers were positive for adipocytes (Figure 14).

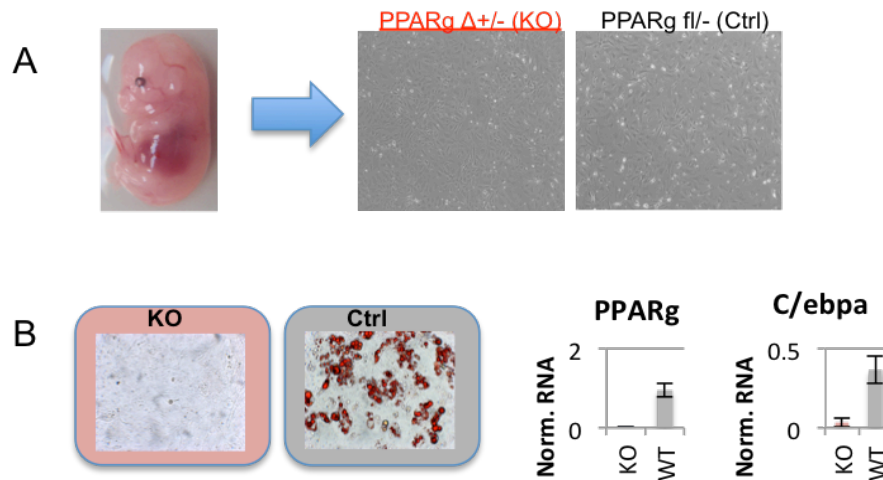


Figure 14. PMEF's isolation and adipocyte differentiation from PPARg KO and control cells derived from the PPARg Sox2Cre genetic background. A) Chemical isolation of PMEF's from individual embryos after genotyping. B) Oil Red O staining after 12 days of PMEF's adipocyte knockout (KO) and heterozygous control (Ctrl) differentiation (left). On the right panel, qPCR data of adipocyte markers are shown (mRNA level was normalized to PPIA).

Induced pluripotent stem cells generation from PPARg null and heterozygous PMEF's.

PMEF's were used to generate iPS cells. First the sleeping beauty transposon system was used. Although, iPS cell lines with the self renewal capability were generate, the adipocyte differentiation efficiency rate was very low in comparison with the embryonic stem cell line used as a technical control. Later, the widely used and highly efficient lentivirus system with a single stem cell cassette was employed for iPS generation. 24 iPS cell lines in total were generated: 12 PPARg null and 12 PPARg heterozygous control cell lines. All of them were passaged during 2 weeks before further experiments. The cell lines stemness was evaluated by alkaline phosphatase staining. According to the morphology of the iPS cell colonies, six cell lines were chosen for further experiments (Figure 15).

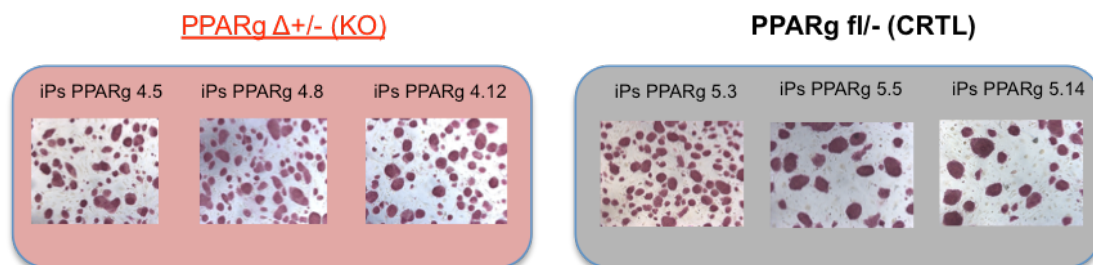


Figure 14. Alkaline phosphatase staining from iPS KO and heterozygous control cell lines after five passages. Staining was performed to evaluate colony morphology and stemness in null (left panel) or control (right panel).

Adipocyte differentiation standardization on embryonic stem cell line.

One of the aims of the generation of PPAR γ null iPS cell lines is to study the molecular control of adipogenesis in a transcriptome and epigenome level. The well characterized and extensively used protocol has two important pitfalls: first the heterogeneity of the culture and second the low efficiency which has been reported (15-30% of adipocytes in the plate). Therefore this type of protocol is not suitable for epigenomic analysis. Furthermore, we set up a highly efficient differentiation protocol for adipogenesis using stem cells adding Ascorbic acid to the adipogenic cocktail and expanding the cells during the differentiation. This new protocol has an efficiency of 80% evaluated by laser scanner cytometry, comparable with other model systems like preadipocyte cell line (3T3-L1) and PMEF's adipocyte differentiation. Importantly, this model follows the highly ordered events in adipogenesis and can be used for next-generation sequencing methods (RNA-seq and ChIP-seq) (Figure 16).

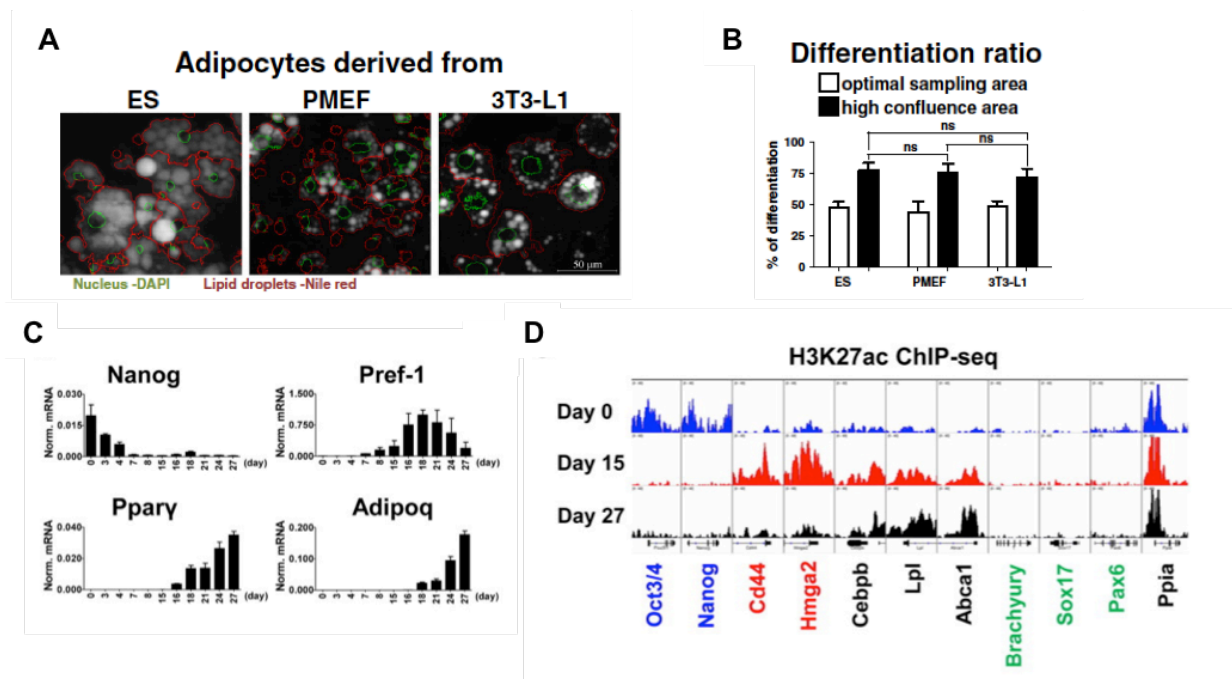


Figure 16. Highly efficient adipocyte differentiation protocol characterization. A) Laser scanning cytometry measurements after Nile red and DAPI staining to evaluate the percentage of differentiation. **B)** Bar graphs of the differentiation ratio. **C)** Gene expression pattern during adipocyte differentiation using different stage markers. **D)** Epigenetic organization in three adipocyte differentiation stages using an active chromatin marker (K27ac). Modified from Cuaranta-Monroy et al., 2014.

PPAR γ knock out and heterozygous control adipocyte differentiation.

After the differentiation of the three selected control iPS cell lines contained high number of adipocytes, meanwhile PPAR γ -KO cell lines were negative for lipid droplets evaluated by Oil Red O staining. These cell lines also showed the expected transcripts levels of different adipocyte differentiation stage markers. For further next-generation analysis we used two cell lines per condition (Figure 17).

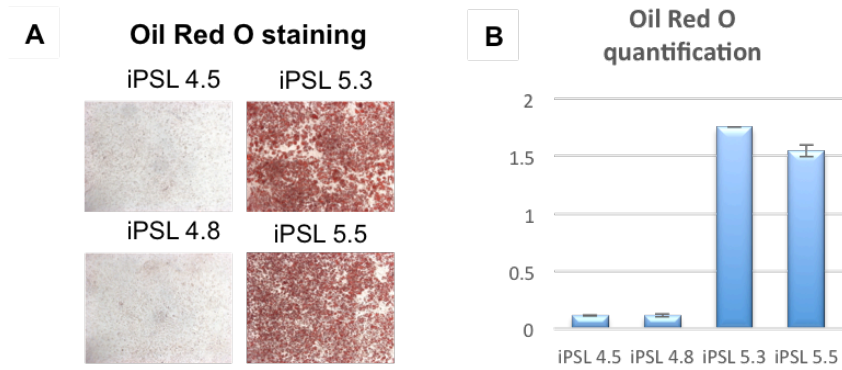


Figure 17. PPARg null and control iPS cell lines adipocyte differentiation. Oil red O staining A) and quantification B) from 27-day cultures.

Transcriptome data from PPARg KO iPS cell lines adipocyte differentiation.

Four time points during adipocyte differentiation from PPARg control and KO iPS cell lines were used to generate RNA-Seq data. Cluster analysis of these samples retrieve 5 clusters: 1. Pparg-independent repression (1265 genes), 2. Pparg-dependent repression (3090 genes), 3. Pparg-dependent up-regulation (1526 genes), 4. Pparg-independent upregulation (972 genes), 5. Pparg-inhibitory effect lost in KO (400 genes). Surprisingly, we could identify an important number of PPARg dependent repressed genes (Figure 18).

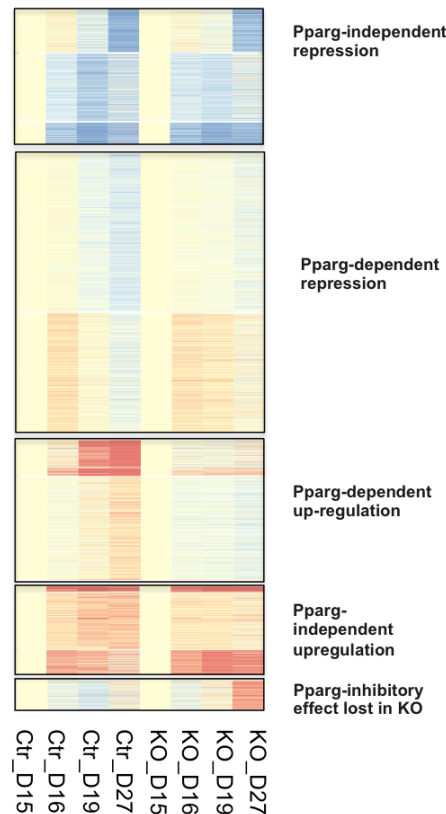


Figure 18. Genome-wide gene expression analysis during iPS cell lines adipocyte differentiation. An unbiased hierarchical cluster analysis and heatmap display of PPARg control and KO iPS cell lines.